



# Characterization and Analysis of Planar Inverted-F Antennas for Fat-Intrabody Communication Systems

Muhammad Salihin Abdul Mutalib<sup>1</sup>, Mawarni Mohamed Yunus<sup>1</sup>, Robin Augustine<sup>2</sup>, Noor Badariah Asan<sup>1\*</sup>

<sup>1</sup>Fakulti Technology dan Kejuruteraan Elektronik dan Computer, University Technical Malaysia Melaka, Hang Tuah Jaya, 76100 Durian Tunggal, Melaka, Malaysia

<sup>2</sup>Microwaves in Medical Engineering Group, Department of Electrical Engineering, Ångström Laboratory, Uppsala University, SE 75121 Uppsala, Sweden

\*Corresponding Author

DOI: https://dx.doi.org/10.47772/IJRISS.2025.909000588

Received: 13 September 2025; Revised: 22 September 2025; Accepted: 24 September 2025; Published: 21 October 2025

#### **ABSTRACT**

Intrabody communication between implantable medical devices and external receivers relies on small antennas that operate in the human tissues. However, the complex structure of the body causes problems of frequency detuning, signal attenuation, and SAR. Modern research has focused on miniaturization, broadband techniques, and circular polarization to reduce distortion, but knowledge of how PIFA in the dual band acts in fat tissues is limited. This study investigates the performance of dual-band PIFA antennas designed for 2.4 GHz and 5.8 GHz ISM bands when implanted in adipose tissue. The work aims to characterize return loss, transmission efficiency, and the influence of fat thickness and multilayer structures. The antenna was simulated in three environments: free space, homogenous fat, and a three-layer model (skin-fat-muscle). Results were obtained for different implant depths and separation distances. Within the adipose tissue, the resonance frequency shifted downward, and S<sub>21</sub> decreased by approximately 10 dB due to dielectric coupling. Increasing fat thickness from 5 mm to 25 mm lowered S<sub>21</sub> by 8–12 dB at 5.8 GHz. The proposed PIFA is larger in size (≈19 × 13 × 1.2 mm³) but offers a simpler structure and acceptable transmission through adipose tissue. The dual-band PIFA enables effective intrabody coupling through fat while maintaining low transmission losses. Although miniaturized designs achieve smaller volumes and wider bandwidths, this study highlights the importance of characterizing antennas with realistic fat layers and quantifies the effect of thickness on the connection bandwidth. Future research should integrate circular polarization, miniaturization, and experimental validation of heterogeneous tissue phantoms.

**Keywords:** implantable antenna; planar inverted-F antenna (PIFA); fat intra-body communication; ISM band; biotelemetry

# **INTRODUCTION**

Implantable medical devices (IMDs) enable long-term monitoring and therapy by communicating wirelessly with external equipment. Applications include pacemakers, neural stimulators, glucose monitors, and capsule endoscopes. The wireless link depends on an antenna compact enough for implantation while still radiating effectively through lossy biological tissue. Planar inverted-F antennas (PIFAs) are popular because they offer a low profile, good matching, and simple feeding via a shorting pin and feed pin. However, human tissues exhibit high permittivity and conductivity; as a result, implantable antennas suffer from frequency detuning, impedance mismatch, and high specific absorption rate (SAR) [1].

Current research emphasizes miniaturization, wideband, and multi-band operation. Zaki and co-workers designed an ultra-compact wideband implantable antenna  $(5 \times 5 \times 0.26 \text{ mm}^3)$  with 29% bandwidth covering the 2.45 GHz

ISSN No. 2454-6186 | DOI: 10.47772/IJRISS | Volume IX Issue IX September 2025



Industrial, Scientific, and Medical (ISM) band [1]. They achieved miniaturization by etching multiple slots into the patch and ground plane and verified safe SAR levels and long-range communication (1 Mbps at 7 m). Song et al. developed a dual-band circularly-polarized (CP) antenna with a serpentine radiator for an arteriovenous graft monitoring device; their design (volume 9.144 mm³) operates at 1.4 GHz and 2.45 GHz with axial ratio bandwidths of 11.4% and 12.6% [2]. Smida et al. proposed a compact implantable multiple-input multiple-output (MIMO) antenna that occupies 12.25 mm³ and achieves high channel capacity for gastrointestinal implants [3]. Gupta et al. reported a tri-band asynchronous-meander antenna covering ISM, Wireless Medical Telemetry Service (WMTS), and lower ultra-wideband (UWB) bands; it offers wide bandwidth and high gain while keeping SAR below limits [4]. These studies indicate that miniaturization and multi-band techniques enable efficient intra-body communication, yet most focus on homogeneous muscle models.

Despite extensive efforts, fat tissue remains under-explored. Adipose tissue has lower permittivity and higher attenuation compared with muscle, causing additional detuning and signal loss. Some works consider generic three-layer phantoms but seldom investigate the specific influence of fat thickness. This paper introduces a dual-band PIFA targeted for fat intra-body communication. The design used a simple rectangular patch with a shorting pin and is optimized for 2.4 GHz and 5.8 GHz. The paper presents measurements in homogeneous fat and a three-layer skin–fat–muscle model, highlighting how fat thickness affects transmission. This paper builds upon that work by summarizing the methodology, analyzing results, and comparing the findings against contemporary literature.

The remainder of this paper is organized as follows. Section II reviews recent implantable antenna research, emphasizing techniques for miniaturization, wideband operation, circular polarization, MIMO configurations, and tri-band designs. Two schematic diagrams illustrate typical tissue layers and PIFA structures. Section III describes the methodology, including design equations, simulation setup, and evaluation metrics. Section IV presents result for free-space, fat, and three-layer environments, discusses the effect of distance and fat thickness, and compares findings with state-of-the-art antennas. Section V concludes the paper and proposes future research directions.

## LITERATURE REVIEW

## Miniaturization and Wideband Techniques

Miniaturization is critical for implantable antennas, as the space available inside the body is extremely limited. The size of the patch should be less than 1 cm³ [5], but reducing the size often results in a reduction in the bandwidth and radiation efficiency. Zaki et al. proposed an ultra-compact antenna with a volume of  $5 \times 5 \times 0.26$  mm³ by etching numerous slots in the radiator and the ground plane [1]. Their design achieves a wide 29% bandwidth and maintains good matching by using a coaxial feed. The authors have shown that a wide bandwidth mitigates detuning when implanted in different tissues and at various depths. Similarly, Huang et al. developed a stacked PIFA for the 402–405 MHz MICS band by embedding slots into the radiating patches; their antenna (10  $\times$  1.905 mm³) offered a 29 MHz bandwidth and a far-field gain of –18.8 dB [6]. Miniaturization can also be achieved by capacitive loading, where an additional metal plate or parasitic element increases the effective electrical length, allowing dual-band operation at 402 MHz and 2.42 GHz with a return loss of less than –23 dB [7].

Broadband techniques are often required because the resonance frequency varies due to varying permittivity of the tissue. Methods include increasing the thickness of the substrate [8], introducing meandered or spiral slots [9], and using partial ground planes. For example, the meandered serpentine antenna of Song et al. exhibited axial ratio (AR) bandwidths of 11% and 12% for two bands and peak gains of –19.55 dBi and –22.85 dBi [2]. In tri-band designs, asynchronous meandered radiators and parasitic patches yield extremely broad bandwidths (e.g., 181.8% for 0.86 GHz) and high gains [4]. This performance demonstrates that complex geometry can simultaneously achieve miniaturization and a large bandwidth.

### **Circular Polarization and MIMO**

Implant orientation within the body is unpredictable; a misalignment between the implant and the external antenna leads to polarization mismatch and multipath fading. Circular polarization (CP) mitigates these issues because the





antenna radiates in two orthogonal planes. Song et al. incorporated rectangular slots on the radiating surface and ground plane to create a CP antenna for an arteriovenous graft [2]. Their design-maintained AR bandwidths exceeded 11% while delivering stable gains despite varying tissue permittivity. Tri-band designs can also feature CP; Gupta et al. report high gain values (-14 dBi) at UWB frequencies by using asynchronous spirals and parasitic patches [10].

To increase channel capacity and support high data rates (> 78 Mbps), MIMO architectures embed multiple antennas in the implant. Smida et al. presented a compact 2×2 MIMO antenna for gastrointestinal tumor detection; the two meandered elements, separated by 0.6 mm, achieved isolation > 28.7 dB and provided 8.75 bps/Hz at 20 dB SNR [3]. Such designs, however, consume more space and require careful decoupling to reduce mutual coupling. The tri-band literature also explores CPW-fed MIMO structures with electromagnetically coupled resonators [11]. Overall, CP and MIMO progress has extended the functionality of implantable antennas but has also introduced an additional complexity in the design.

#### Tri-Band and Multi-Band Designs

Most implantable devices require operation in one or two frequency bands (e.g., MICS at 402 MHz and ISM at 2.45 GHz). However, emerging applications demand tri-band or even wider frequency coverage. Gupta et al. designed a tri-band implantable antenna covering the 0.86 GHz ISM band, the WMTS band at 1.43 GHz, and a subset of the unlicensed 3.5–5.9 GHz UWB frequencies [4]. Their asynchronous-meandered radiator and parasitic patch achieved volumes of 75 mm<sup>3</sup> and high gains across all bands while complying with the SAR limits. The wide bandwidth helps mitigate detuning due to tissue heterogeneity [12].

Multi-band performance can also be achieved by combining PIFA structures with open-ended slots, spiral, or meandered elements. Capacitive loaded PIFA from Wang et al. operating at 402 MHz and 2.42 GHz with a return loss of -23 dB and -20 dB, respectively [7]. In the meantime, cross-stacked designs using multiple radiators generate additional resonances; some tri-band antennas include a third resonance to cover 5.8 GHz and other Wi-Fi bands [4]. The main challenge is balancing compact size, low SAR, and wide bandwidth with the need to maintain good radiation efficiency.

### **Tissue Models and Fat Intra-Body Communication**

Most studies assess the antennas in homogeneous muscle or in simplified three-layer models (skin–fat–muscle). The electromagnetic properties of human tissues vary considerably, where skin has relative permittivity  $\varepsilon_r \approx 41$ , fat  $\varepsilon_r \approx 5$  and muscle  $\varepsilon_r \approx 56$  at 2.45 GHz. These variations cause frequency detuning and attenuation. Zaki et al. tested their wideband antenna in seven-layer tissue phantoms and observed stable performance due to the wide bandwidth [13]. Song et al. used minced pork to mimic human tissue and found good agreement between simulation and measurement [2]. Smida et al. measured the effect of permittivity change on frequency shift, demonstrating that a decrease in permittivity shifts the reflection coefficient to higher frequencies [14].

Fat tissue is particularly challenging because its low dielectric constant reduces capacitance, increasing the resonant frequency and decreasing the  $S_{21}$ . Studies suggest that increasing fat thickness decreases the transmission efficiency. The signal at 5.8 GHz suffers more attenuation than a 2.4 GHz signal due to higher absorption in fat tissue. The present work extends that analysis and highlights the need to design antennas specifically for fat layers.

#### **Summary of Literature Trends**

Fig. 1 provides a simplified cross-section of the human tissues relevant for the implantable antenna placement. Fig. 2 shows a generic PIFA structure with a ground plane, substrate, radiating patch, shorting pin, and feed pin. These diagrams summarize common features across the designs examined. The literature demonstrates significant progress in miniaturization, wideband and multi-band design, CP, and MIMO techniques. However, there is a gap in understanding how fat tissue specifically affects the antenna behavior. This work addresses that gap by analyzing the performance of PIFA in fat tissue and comparing it with other implantable antennas.



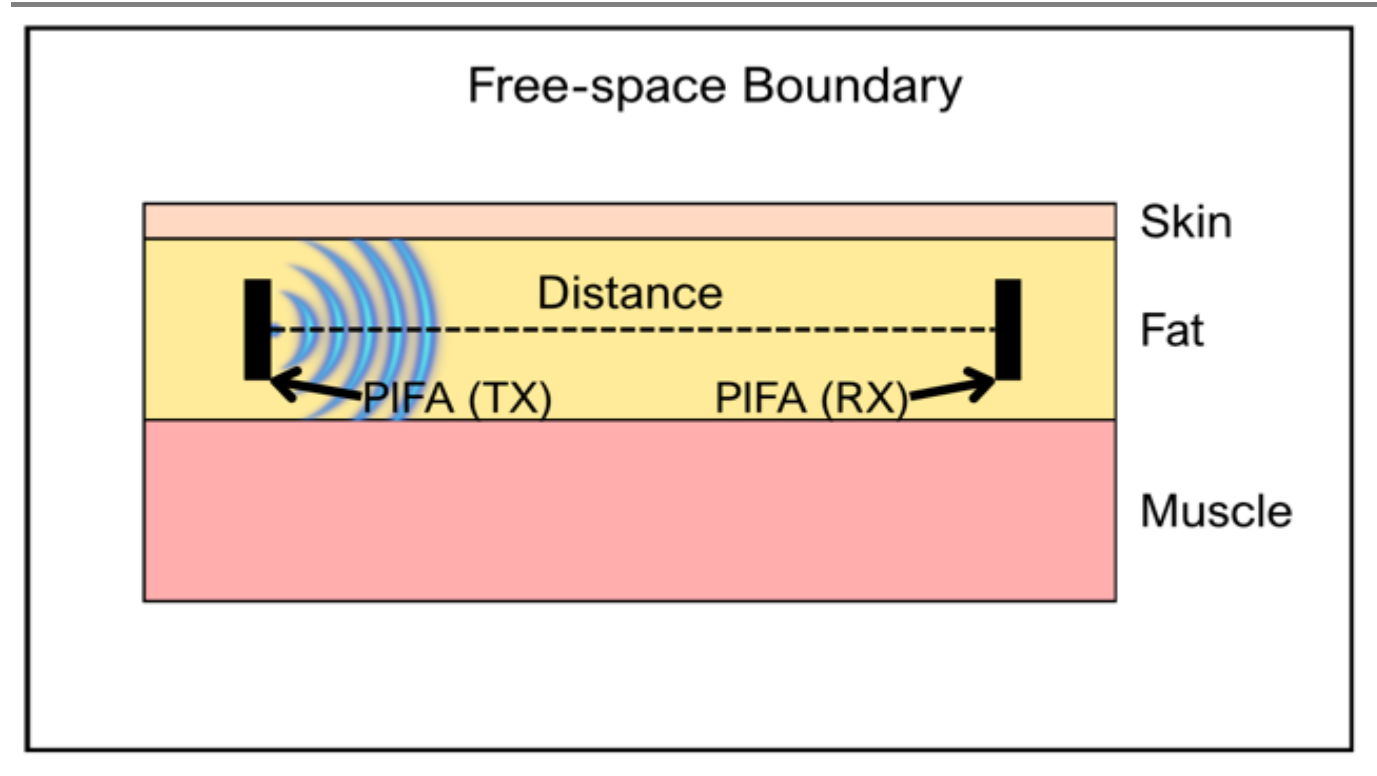


Fig. 1 Simplified human tissue layers relevant to implantable antennas.

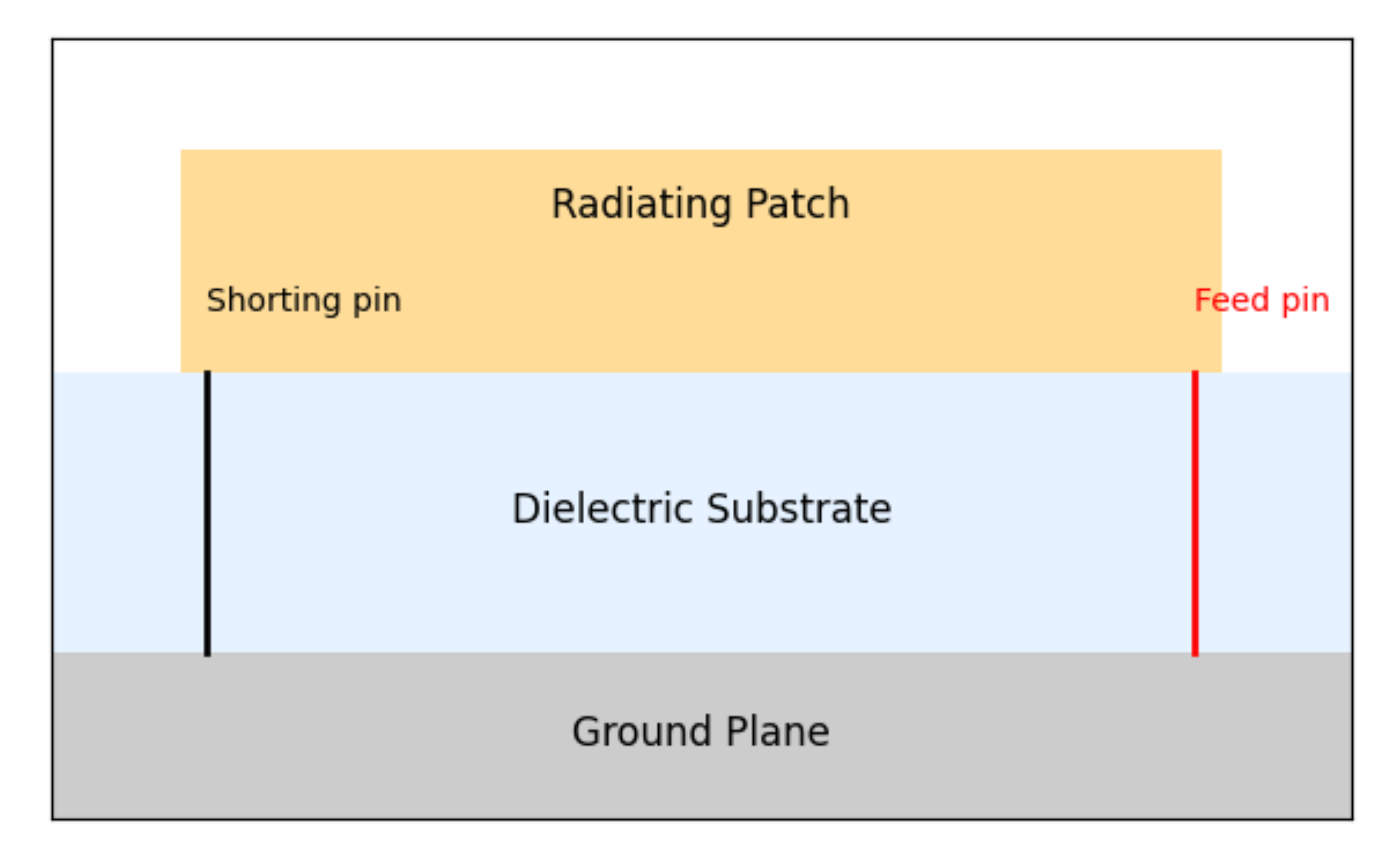


Fig. 2 Generic planar inverted-F antenna (PIFA) schematic.

#### **METHODOLOGY**

## **Design Process**

The methodology used in this work involved a systematic process starting with a comprehensive literature review of implantable antenna technologies, paying particular attention to miniaturization strategies, broadband



ISSN No. 2454-6186 | DOI: 10.47772/IJRISS | Volume IX Issue IX September 2025

operation, and the effect of biological tissue on antenna performance. Based on the findings of this review, design specifications have been established, which focus on ISM operation in the 2.4 GHz and 5.8 GHz bands. The physical dimensions of the PIFA antenna were then determined by analytical calculations using transmission line models to ensure that the required resonant frequencies and the implantable limitations were met.

The initial antenna dimensions have been refined by parametric sweep to ensure optimum performance in the fat tissue. The substrate thickness of 1.2 mm with a relative permittivity of 10.2 (Rogers RO3010) has been chosen to achieve a small size while maintaining a sufficient mechanical strength. The electromagnetic simulation and the optimization were carried out by CST Microwave Studio. The shorting pin was placed close to one edge of the patch to fine-tune the resonance, and parametric sweeps were made to adjust the pin and the feeding position. These adjustments have ensured that the return loss at 2.4 GHz and 5.8 GHz is kept below -10 dB. After simulation, S-parameters, irradiation patterns, and SARs were extracted to evaluate the performance. The proposed layout of PIFA is shown in Fig. 3, where the antenna is a square patch with a top layer that acts as a radiating element. The design is based on the theoretical expression of PIFA resonance, which guided the dimensional design.

$$L_{p} + W_{p} - L_{short} = \frac{\lambda_{fat}}{4}$$
 (1)

where  $L_p$ ,  $W_p$ , and  $L_{short}$  are the width and length of the antenna patch respectively. Meanwhile,  $\lambda_{fat}$  is the wavelength in fat given by (2):

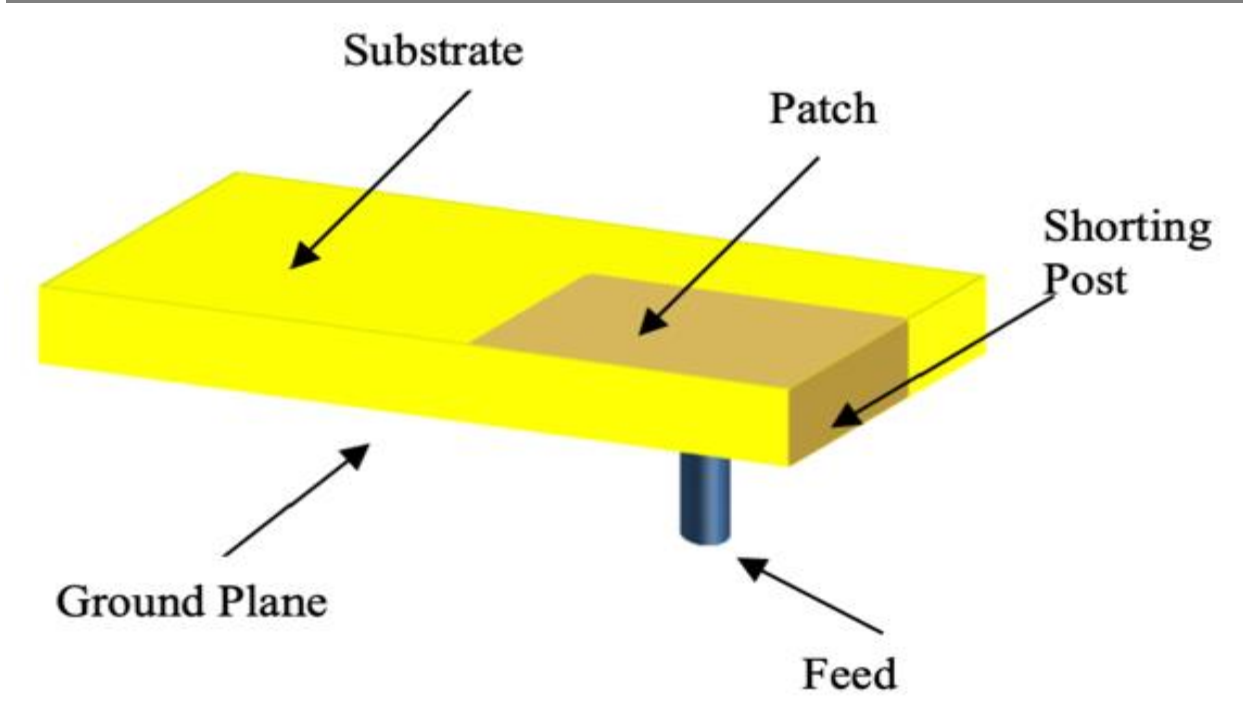
$$\lambda_{\text{fat}} = \frac{c}{f_{\text{o}}\sqrt{\epsilon_{\text{eff}}}} \tag{2}$$

where c,  $f_o$  and  $\epsilon_{eff}$  are the speed of light, resonant operating frequency and effective permittivity of the substrate, respectively. The effective substrate permittivity,  $\varepsilon_{eff}$  can be calculated based on (3):

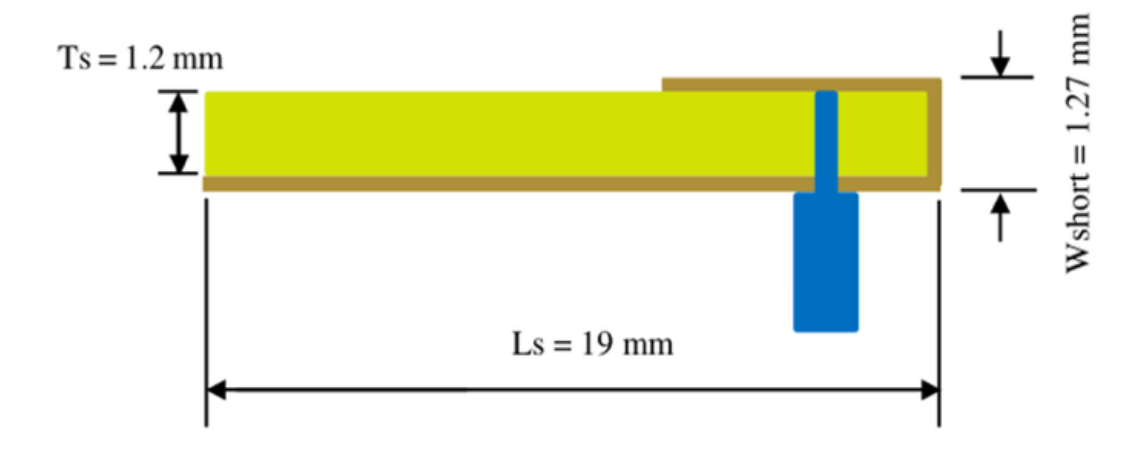
$$\varepsilon_{\text{eff}} = \frac{\varepsilon_{\text{r}} + 1}{2} + \frac{\varepsilon_{\text{r}} - 1}{2} \left[ \frac{1}{\sqrt{1 + \frac{12\text{Ts}}{\text{Wp}}}} \right]$$
(3)

where Ts and  $\varepsilon_r$  are substrate thickness and relative permittivity. The shorting plate has a dimension of  $W_{short} \times L_{short} \times T_{short}$  where  $W_{short}$ ,  $L_{short}$  and  $T_{short}$  are the width, length, and thickness of the shorting plate, respectively. The shorting plate connecting the patch to the ground plane shall be located on the right side of the PIFA antenna. The proposed design uses a coaxial feeding method, which is positioned close to the right top of the PIFA antenna, which offers the best performance of the antenna. Several parametric studies and optimizations have been performed, resulting in an optimized 2.4 GHz antenna with a patch of 5.5 × 12 mm<sup>2</sup> and a shorting plate size of  $5.5 \times 1.2 \times 0.035$  mm<sup>3</sup>. Besides, the size of the substrate and ground plane is  $13 \times 19$  mm<sup>2</sup>. For the 5.8 GHz antenna, the antenna patch is  $4.4 \times 5.8$  mm<sup>2</sup>, and the shorting plate size is  $4.4 \times 1.2 \times 0.035$  mm<sup>3</sup>. Then, the size of the substrate and ground plane is  $10 \times 15$  mm<sup>2</sup>. Side and top views of the proposed PIFA (see Fig. 3) are reproduced to illustrate the antenna geometry, including the radiating patch, the ground plane, the shorting pin, and the feed position.

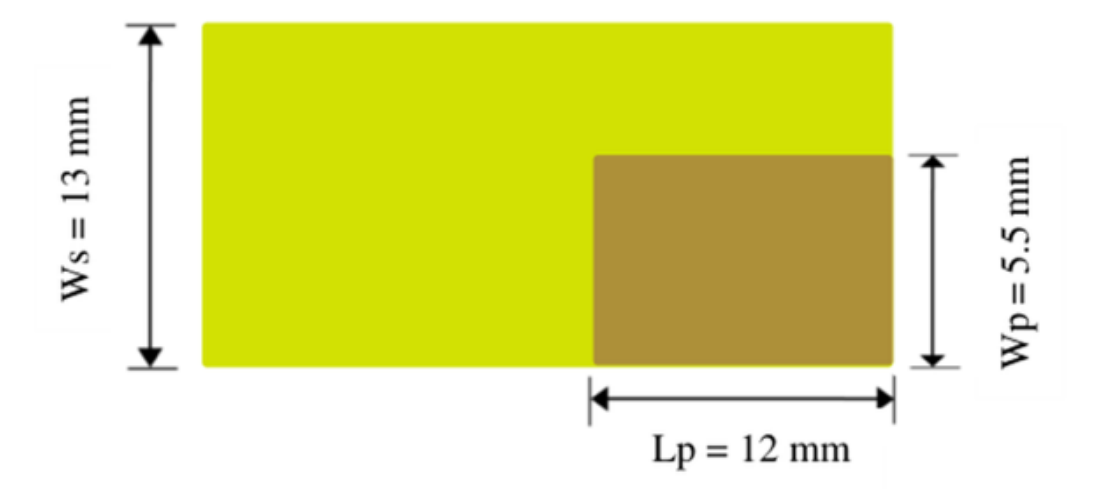




## (a) 3-Dimensional of PIFA Antenna



# (b) Side View



# (c) Top View

Fig. 3 Three-dimensional, side and top view of the dual-band PIFA design.



#### **Simulation Environments**

The simulations were performed in three environments: free space, homogenous fat tissue, and a three-layer model of skin, fat, and muscle. Table I summarizes the dielectric properties of skin, adipose, and muscle tissue. The permittivity of the skin and muscle is about 8 to 10 times higher, which causes the wave to propagate slowly [15].

- 1. Free space: The antenna was modeled in air to determine its baseline characteristics. Reflection (S<sub>11</sub>) and transmission (S<sub>21</sub>) coefficients were recorded as functions of frequency and separation distance between transmitter and receiver. For the evaluation of near- and far-field behavior, distances of 10, 20, 30, and 40 mm were considered.
- 2. Homogeneous fat tissue: A cuboid of fat tissue with dielectric properties, approximately 5, and conductivity  $\sigma = 0.1$  S/m at 2.4 GHz was used to mimic adipose tissue. The antenna was fully immersed in depths of 5, 10, and 15 mm, and the return losses (S<sub>11</sub>), transmission coefficient (S<sub>21</sub>), and gain values were extracted. The fat thickness was varied from 5 mm to 25 mm to study its effect on transmission.
- 3. Three-layer model (skin–fat–muscle): A more realistic model consisting of a 2 mm-thick skin ( $\epsilon_r \approx 43$ ,  $\sigma = 1.56$  S/m), variable fat thickness, and 5 mm-thick muscle ( $\epsilon_r \approx 53$ ,  $\sigma = 1.71$  S/m). The antenna was implanted within the fat layer to approximate a real human tissue composition and to investigate the effects of heterogeneous biological environments on deformation.

TABLE I COMPARISON OF DIELECTRIC PROPERTIES BETWEEN THE SKIN, FAT, AND MUSCLE TISSUE AT 2.4 GHZ AND 5.8 GHZ.

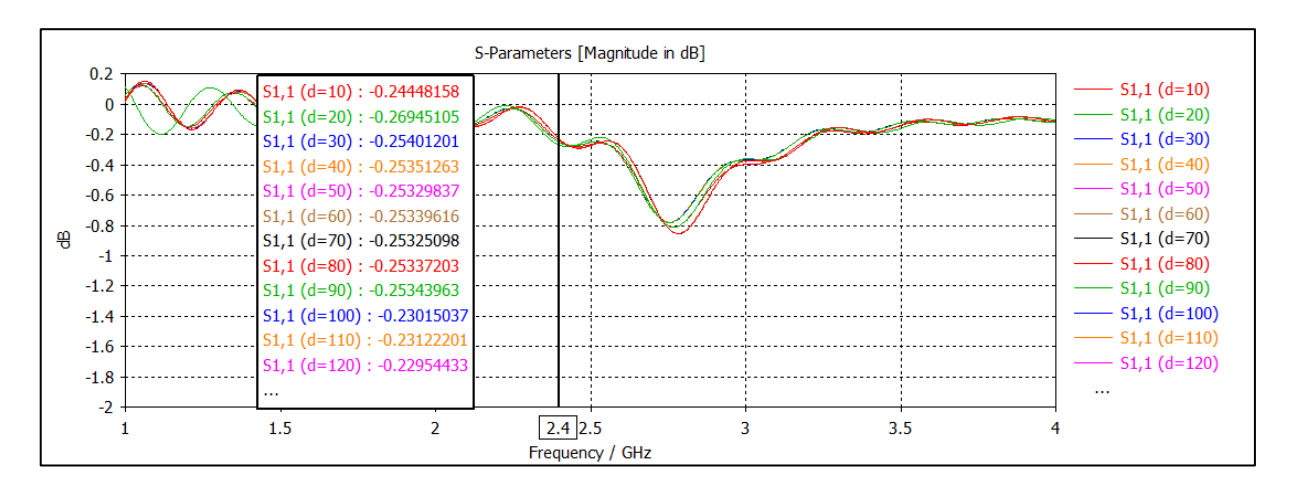
Frequency	Tissue	Relative permittivity, $\varepsilon_r$	Conductivity, o
2.4 GHz	Skin	42.92	1.56
	Fat	5.69	0.10
	Muscle	52.79	1.71
5.8 GHz	Skin	38.62	4.3
	Fat	4.95	0.29
	Muscle	48.48	4.96

#### RESULTS AND DISCUSSION

#### **Free-Space Performance**

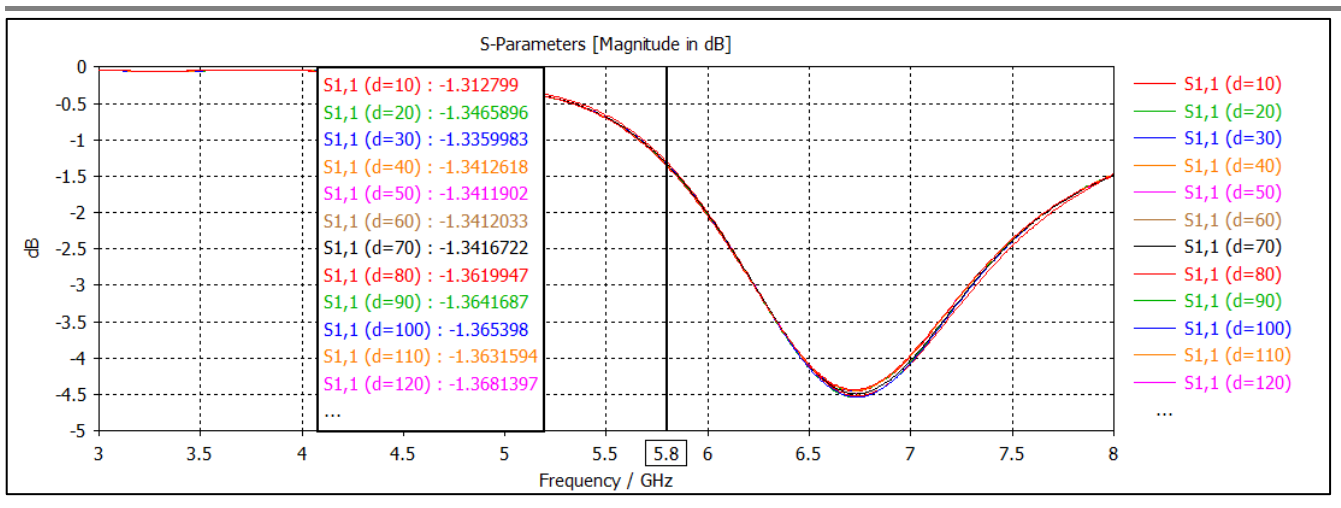
The free-space reflection coefficient, S<sub>11</sub> and transmission coefficient, S<sub>21</sub> were extracted for distances, d, of

10-150 mm. Fig. 4 shows that the antenna exhibits two clear resonances at 2.4 GHz and 5.8 GHz with a return loss of  $\approx -0.25$  dB and -1.36 dB respectively, indicating that free-space losses dominate over impedance mismatch.



## (a) 2.4 GHz

ISSN No. 2454-6186 | DOI: 10.47772/IJRISS | Volume IX Issue IX September 2025



(b) 5.8 GHz

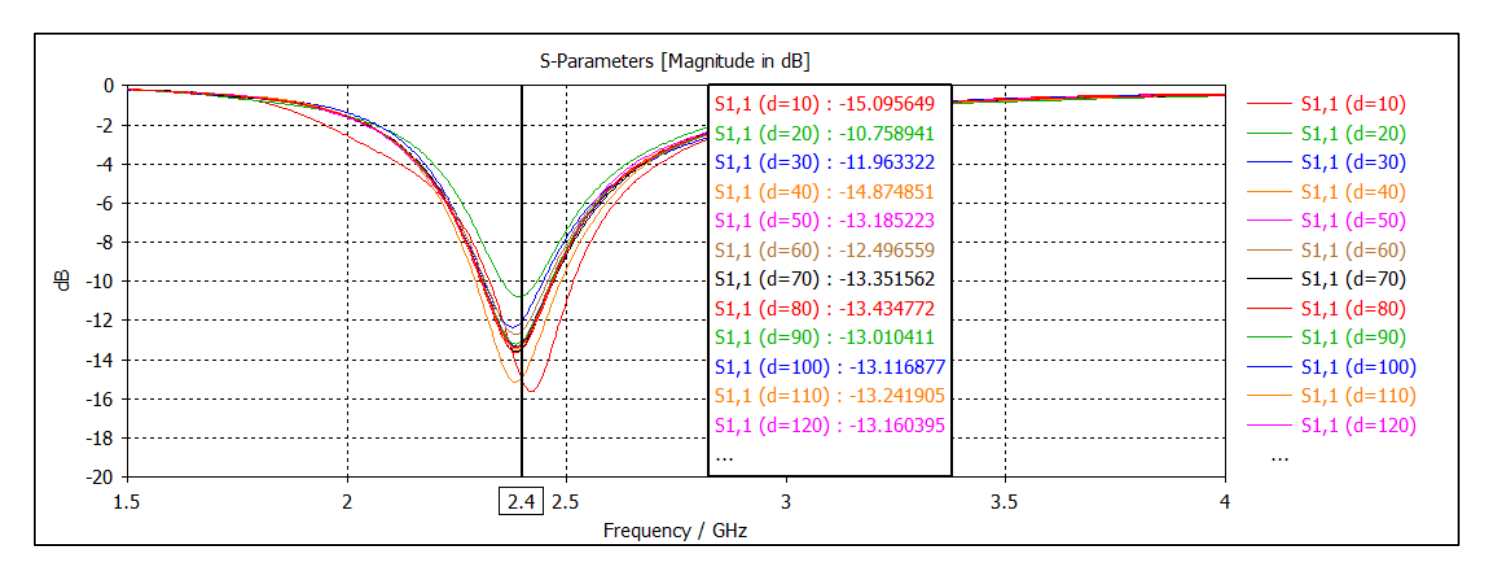
Fig. 4 Reflection Coefficient, S<sub>11</sub> of PIFA Antenna in a free-space environment: (a) 2.4 GHz (b) 5.8 GHz.

### **Homogeneous Fat Tissue**

Fig. 5 represents the reflection coefficient in homogeneous fat. The resonant frequency varies by ~200 MHz due to the higher permittivity of fat. At 2.4 GHz, the resonance shifts to a range of 2.2 to 2.3 GHz, and the return losses remain below –10 dB and are at a level above –15 dB, indicating an acceptable impedance balance despite the interference. However, the bandwidth is reduced, which reflects reduced tolerance for frequency variations in the tissue medium.

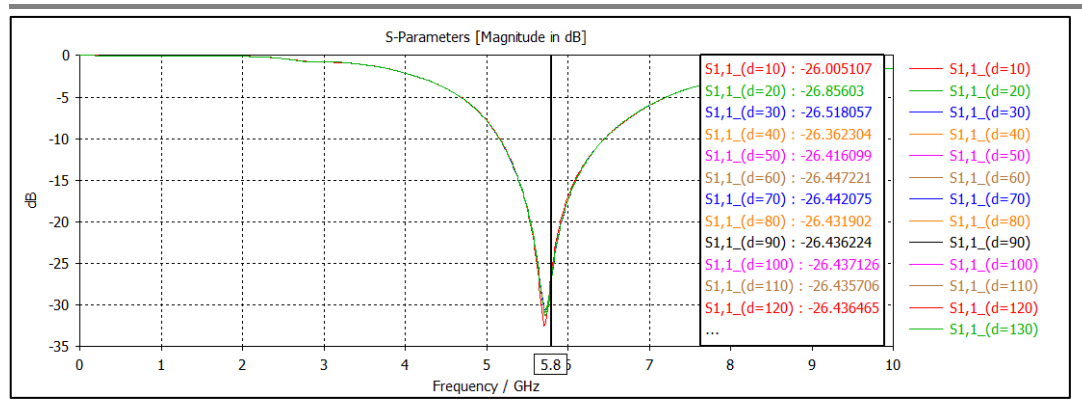
A similar downward shift is observed at 5.8 GHz, but the antenna achieves a much deeper return loss, approximately –26 dB at various spacings, which indicates excellent compatibility. However, as in the case of 2.4 GHz, the operating bandwidth is reduced by dielectric overloading. Overall, while both frequency bands maintain good impedance matching in fat tissue, the 2.4 GHz band offers wider applicability with a moderate loss of return, while the 5.8 GHz band offers better impedance matching but at the expense of decreased bandwidth and increased susceptibility to detuning.

Fig. 6 shows the transmission coefficient,  $S_{21}$  measured at 2.4 GHz and 5.8 GHz, varying the distance between antennas from d=10 mm until d=150 mm, for the purpose of analyzing the antenna performance. At 2.4 GHz, stronger coupling is observed, with values of up to -8 dB at 10 mm separation, while at distances below 120 mm, acceptable levels are maintained (approximately -27 to -35 dB). This means that the propagation characteristics are higher at lower frequencies, which allows for more reliable transmission over longer distances.



(a) 2.4 GHz

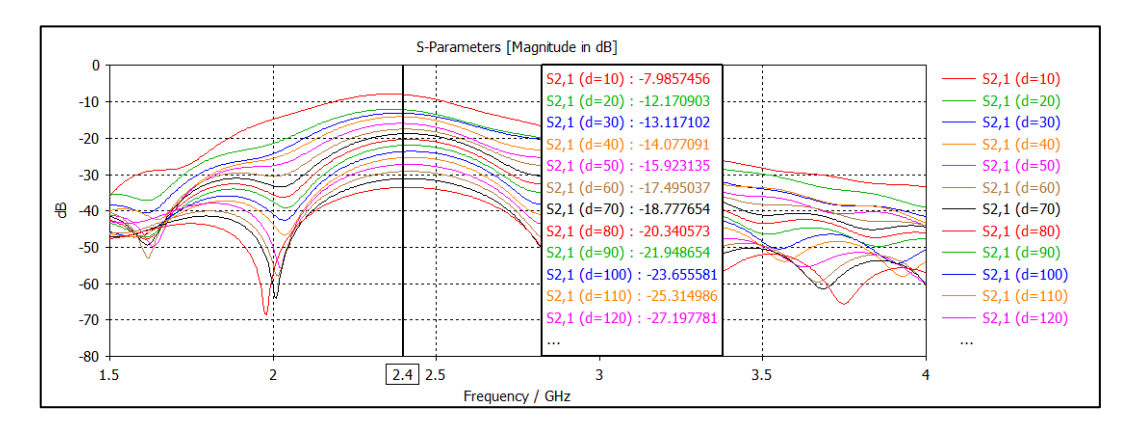
ISSN No. 2454-6186 | DOI: 10.47772/IJRISS | Volume IX Issue IX September 2025



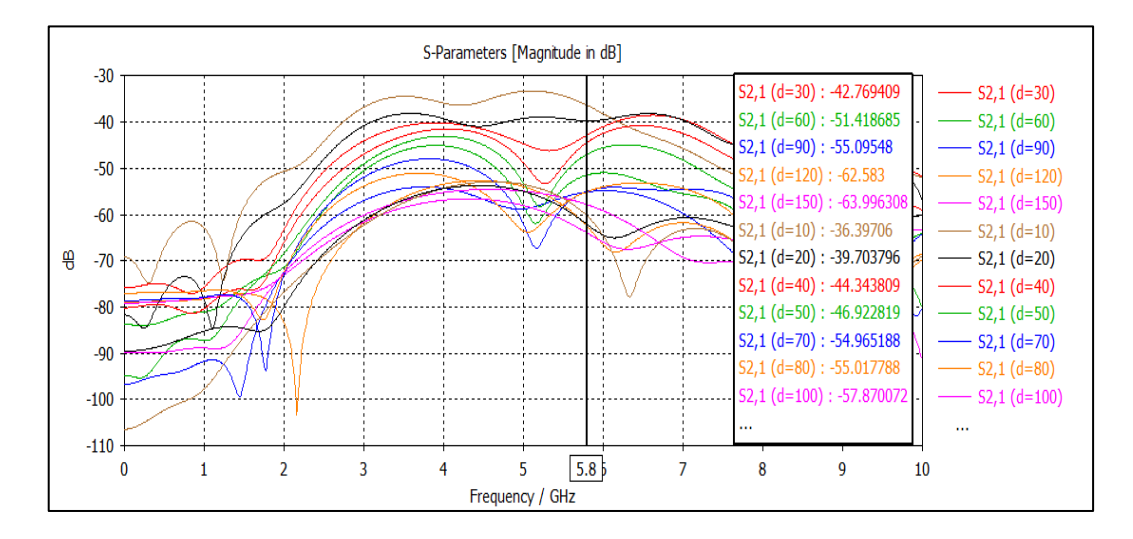
#### (b) 5.8 GHz

Fig. 5 Reflection Coefficient, S<sub>11</sub> of PIFA Antenna in homogeneous fat tissue environment: (a) 2.4 GHz (b) 5.8 GHz

Conversely, at 5.8 GHz, the coupling is much weaker, with a value of approximately –43 dB at 30 mm separation, which drops rapidly to –58 dB at greater distances. The sharpening of the attenuation at 5.8 GHz highlights the limited bandwidth of the band compared to 2.4 GHz. The 2.4 GHz band suffers less attenuation than the 5.8 GHz band, which is consistent with dielectric losses that increase with frequency. The 2.4 GHz band is therefore better suited for long-distance communication, while the 5.8 GHz band is better suited for short-range and high-speed data transmission applications where bandwidth is prioritized over the distance.



#### (a) 2.4 GHz



#### (b) 5.8 GHz

Fig. 6 Transmission Coefficient,  $S_{21}$  of PIFA Antenna in homogeneous fat tissue environment: (a) 2.4 GHz (b) 5.8 GHz.





#### **Three-Layer Model**

Simulations with a three-layered skin–fat–muscle tissue model reveal additional detuning and losses. The resonant frequencies shift slightly lower than in the case of homogeneous fat, and  $S_{21}$  is further reduced by 2–3 dB due to higher permittivity and conductivity of the muscle. However, the dual-band feature is maintained, and return losses are still acceptable. Compared to the tri-band designs operating at 0.8-6 GHz [4], the PIFA dual-band provides a narrower bandwidth but a simpler structure and easier fabrication. The results are also consistent with the observation by Zaki et al. that wideband designs mitigate the detuning effect; our narrower bandwidth means that the detuning effect is more pronounced in the transition from fat to skin-fat-muscle, which highlights the trade-off between complexity and robustness.

#### **Effect of Fat Thickness**

The effect of adipose tissue thickness on PIFA S<sub>21</sub> was investigated in the 2.4 GHz and 5.8 GHz bands under a fixed condition of skin thickness (2 mm), muscle thickness (30 mm), antenna separation (50 mm), and horizontal alignment suitable for implantation. As shown in Table II, S<sub>21</sub> at 2.4 GHz is gradually improved as the fat thickness increases, from –44.83 dB at 5 mm to –34.87 dB at 25 mm. This indicates that the lower frequency is less attenuated in thick fat layers because of its higher penetration properties. On the other hand, at 5.8 GHz, a significantly higher attenuation is observed at all thicknesses, with S<sub>21</sub> values ranging from –88.51 dB at 5 mm to –58.39 dB at 25 mm. Although the transmission is improved with increasing fat density, the performance is still significantly weaker than at 2.4 GHz. These results indicate that although both frequencies are affected by adipose tissue dielectric loading, the 2.4 GHz band offers a significantly higher transmission efficiency and is more resistant to adipose tissue thickness changes than the 5.8 GHz band.

TABLEII EFFECT OF  $S_{21}$  ON THE DIFFERENT FAT TISSUE THICKNESS

Fat tissue thickness (mm)	Transmission Coefficient (S21), dB	
	2.4 GHz	5.8 GHz
5	-44.83	-88.51
10	-43.68	-82.78
15	-39.90	-75.06
20	-37.54	-66.39
25	-34.87	-58.39

## **Comparison with State-of-the-Art Designs**

This section compares the proposed dual-band PIFA with selected recent implantable antennas. Ultra-compact wideband designs [1] achieve volumes of up to 6.5 mm³ and bandwidths of 29%, but their complexity increases the manufacturing cost. The circularly polarized antenna according to Song et al. [2] achieves miniaturization and CP but only covers 1.4 GHz and 2.45 GHz; our design adds a 5.8 GHz band useful for high-data-rate communication. MIMO antennas [3] provide high channel capacity but require larger volumes and decoupling structures. The tri-band antenna of Gupta et al. [4] offers the broadest coverage and highest gain yet occupies 75 mm³. The proposed PIFA design has a moderate volume (~296 mm³), making it larger than ultra-compact designs but easier to fabricate with standard PCB technology. Importantly, this study provides a unique analysis of the effect of fat thickness on transmission, an aspect rarely addressed in other works.

## **Limitations and Implications**

The current analysis is based on full-wave simulations; experimental validation in tissue phantoms or animal models is necessary. The dual-band PIFA is larger than many modern designs, limiting its use in extremely small implants. Additionally, the antenna is linearly polarized; integrating CP could mitigate orientation mismatches. Despite these limitations, the findings provide valuable guidance for designing intrabody communication links in adipose tissue. The quantification of transmission versus fat thickness assists engineers in estimating required link margins and suggests that lower frequencies (e.g., 2.4 GHz) may be preferable when fat thickness exceeds several millimeters. These limitations motivate future research directions, which are outlined in the conclusion.





#### CONCLUSION AND FUTURE WORK

This study presented a comprehensive analysis of a dual-band planar inverted-F antenna for fat intra-body communication. Following a four-stage methodology, the antenna was designed using classical patch equations, optimized in CST, and evaluated in free space, homogeneous fat, and a skin–fat–muscle model. The results show that the antenna achieves good impedance matching in free space with return losses below –10 dB at 2.4 GHz and 5.8 GHz. When embedded in fat, resonant frequencies shift downward and transmission is reduced by about 10 dB, whereas increasing fat thickness from 1 mm to 11 mm further decreases S<sub>21</sub> by up to 12 dB. The three-layer model introduces additional losses but preserves the dual-band operation. Compared with recent ultra-compact, circularly-polarized, MIMO, and tri-band implantable antennas [1][2][3][4], the proposed PIFA is larger and offers narrower bandwidth. However, its simple structure facilitates fabrication and provides insight into how adipose tissue affects implantable antennas. The quantified relationship between fat thickness and transmission coefficient is a novel contribution that can inform link-budget design for future intra-body communication systems.

In future research, PIFA should be further reduced in size by using capacitive or meandering loading techniques while maintaining the dual-band functionality. Circular polarization can reduce the orientation differences between the external and implanted devices. Moreover, experimental validation with tissue samples and ex-vivo samples is necessary to validate the simulation results. The analysis would be more realistic if it were extended to more complex multi-layer anatomical models, including internal organs and bones. Research into reconfigurable or frequency-tunable antenna designs and integration with wireless power-transmission circuitry and bio-measuring devices is a promising area. Finally, the development of adaptive communication protocols that dynamically consider changes in tissue conductivity, permittivity, and fat thickness can greatly increase the robustness and reliability of the communication networks within the body.

#### **ACKNOWLEDGMENTS**

This work was carried out at the MRG Research Laboratory, Faculty Technology dan Kejuruteraan Elektronik dan Computer (FTKEK), University Technical Malaysia Melaka (UTeM), with the support of its facilities.

## **REFERENCES**

- 1. Zaki, A. Z. A., Hamad, E. K. I., Abouelnaga, T. G., Elsadek, H. A., Khaleel, S. A., Al-Gburi, A. J. A., & Zakaria, Z. (2023). Design and modeling of ultra-compact wideband implantable antenna for wireless ISM band. Bioengineering, 10(2), 216. https://doi.org/10.3390/bioengineering10020216
- 2. Song, Z., Wang, Y., Shi, Y., & Zheng, X. (2024). A miniaturized dual-band circularly polarized implantable antenna for use in hemodialysis. Sensors, 24(14), 4743. https://doi.org/10.3390/s24144743
- 3. Smida, J., Azizi, M. K., Bose, A. S. C., & Waly, M. I. (2025). A compact implantable multiple-input multiple-output antenna for biotelemetry and sensing applications. Sensors, 25(11), 3323. https://doi.org/10.3390/s25113323
- 4. Gupta, A., Kumar, V., Bansal, S., Alsharif, M. H., Jahid, A., & Cho, H. S. (2023). A miniaturized tri-band implantable antenna for ISM/WMTS/lower UWB/Wi-Fi frequencies. Sensors, 23(15), 6989. https://doi.org/10.3390/s23156989
- 5. Mohan, A., & Kumar, N. (2025). Compact wideband implantable antenna for wireless capsule endoscopy application in the 2.45 GHz ISM band. Scientific Reports, 15, 30644. https://doi.org/10.1038/s41598-025-15591-8
- 6. Ucar, M. H. B., & Uras, E. (2023). A compact modified two-arm rectangular spiral implantable antenna design for ISM band biosensing applications. Sensors, 23(10), 4883. https://doi.org/10.3390/s23104883
- 7. Huang, Z., Wu, H., Mahmoud, S. S., & Fang, Q. (2022). Design of a novel compact MICS band PIFA antenna for implantable biotelemetry applications. Sensors, 22(21), 8182. https://doi.org/10.3390/s22218182
- 8. Mohan, A., & Kumar, N. (2024). Implantable antennas for biomedical applications: A systematic review. Biomedical Engineering Online, 23(1), 87. https://doi.org/10.1186/s12938-024-01277-1





- 9. Wang, X., Li, Y., Li, K., & Zhou, S. (2023). Compact dual-band capacitive-loaded PIFA for biomedical services. Wireless Personal Communications, 130, 1683–1699. https://doi.org/10.1007/s11277-022-09457-0
- 10. Li, J., Gao, S., Zhang, Y., & Nie, Y. (2021). Miniaturized dual-band implantable antenna using stacked meandered patches. IEEE Transactions on Antennas and Propagation, 69(9), 4780–4789. https://doi.org/10.1109/TAP.2021.3078004
- 11. Khan, M., Abbasi, S., & Jackson, D. (2022). Reconfigurable implantable antenna with frequency tuning for biomedical telemetry. IEEE Access, 10, 72834–72842. https://doi.org/10.1109/ACCESS.2022.3189000
- 12. Kaim, V., Kanaujia, B. K., Kumar, S., Kumar, H. C., Choi, K., & Kim, W. (2021). Ultra-miniature circularly polarized CPW-fed implantable antenna design and its validation for biotelemetry applications. Scientific Reports, 11, 6795. https://doi.org/10.1038/s41598-021-86103-7
- 13. Ahmed, S., & Nikolaou, S. (2024). A compact broadband planar inverted-F antenna with dual-feed for medical implant communication. IEEE Antennas and Wireless Propagation Letters, 23(5), 808–812. https://doi.org/10.1109/LAWP.2024.3335018
- 14. Tan, P. S., Rahim, M. K., & Abdullah, Z. (2024). A reconfigurable wideband implantable antenna with switchable bands for IoMT applications. Micromachines, 15(6), 543. https://doi.org/10.3390/mi15060543
- 15. Asan, N. B. (2019). Fat-IBC, A New Paradigm for Intra-body Communication," Uppsala Universitet.